

# Determinative Role of the Jahn-Teller Disorder in the Raman Scattering of Mixed-Valence Manganites

M. N. Iliev<sup>1</sup>, M. V. Abrashev<sup>2</sup>, V. N. Popov<sup>2</sup>, V. G. Hadjiev<sup>1</sup>

<sup>1</sup>*Texas Center for Superconductivity and Advanced Materials,  
University of Houston, Houston, Texas 77204-5002*

<sup>2</sup>*Faculty of Physics, University of Sofia, 1164 Sofia, Bulgaria*  
(Dated: December 2, 2024)

The mixed-valence perovskitelike manganites are characterized by unique interrelation of Jahn-Teller distortions, electric and magnetic properties. The Jahn-Teller distortion follows the  $\text{Mn}^{3+} \rightarrow \text{Mn}^{4+}$  charge transfer with some delay. Its development depends on the lifetime of Mn in  $3+$  state, governed by the  $\text{Mn}^{4+}/\text{Mn}^{3+}$  ratio and magnetic correlation. The non-coherence of Jahn-Teller distortions in orthorhombic mixed-valence manganites and rhombohedral  $\text{RMnO}_3$  ( $R$  = rare earth) results in oxygen disorder. We demonstrate that the Raman spectra in this case are dominated by disorder-induced bands reflecting the oxygen partial phonon density of states (PDOS). The PDOS origin of the main Raman bands in insulating phases of such compounds is evidenced by the similar lineshape of experimental spectra and calculated smeared PDOS and disappearance of the PDOS bands in ordered ferromagnetic metallic phase.

PACS numbers: 78.30.Ly, 63.50.+x, 63.20.Mt, 71.30.+h

The structure of perovskitelike manganites  $\text{A}_{1-x}\text{A}'_x\text{MnO}_3$  ( $A$  - trivalent rare-earth,  $A'$  - divalent alkaline-earth) differs from that of an ideal cubic perovskite by mainly in-phase or out-of-phase rotations of  $\text{MnO}_6$  octahedra around some of the cubic axes [1] and stretching distortions of  $\text{Mn}^{3+}\text{O}_6$  (but not  $\text{Mn}^{4+}\text{O}_6$ ) octahedra due to the Jahn-Teller (JT) effect. At a microscopic level the structure has exact translational symmetry in only few cases, such as the orthorhombic phase ( $Pnma$ ) of  $\text{LaMnO}_3$  and  $\text{CaMnO}_3$  or the charge and orbital ordered (COO) phase ( $P2_1/m$ ) of  $\text{La}_{0.5}\text{Ca}_{0.5}\text{MnO}_3$ . In the general case, the real local structure of mixed valence  $\text{A}_{1-x}\text{A}'_x\text{MnO}_3$  *a priori* differs from the averaged one (as determined by diffraction studies) due to the random distribution of  $\text{A}^{3+}$  ( $\text{A}'^{2+}$ ) and  $\text{Mn}^{3+}$  ( $\text{Mn}^{4+}$ ) ions, respectively. The translational symmetry in this case is only an approximation and the effects of atomic disorder have to be accounted for.

The static random distribution of  $\text{A}^{3+}$  and  $\text{A}'^{2+}$  has little effect on the conductivity and magnetic properties as these ions do not participate in the electron transfer mechanism. In contrast, the random distribution of  $\text{Mn}^{3+}$  and  $\text{Mn}^{4+}$  at the B-sites determines to a great extent the electronic transport and magnetic ordering. The  $\text{Mn}^{3+}/\text{Mn}^{4+}$  charge and orbital disorder results in structural disorder, too. The latter disorder is mainly due to the difference of the bond lengths in non-coherently distributed  $\text{Mn}^{3+}\text{O}_6$  and  $\text{Mn}^{4+}\text{O}_6$  octahedra. While, upon change of the Mn valence, the oxygen atoms shift significantly from their positions in the averaged structure, the Mn ions remain practically unshifted.

The effects of static atomic disorder have intensively been investigated on the examples of non-crystalline (amorphous) materials. Most of their properties, e.g. the mechanism of conductivity, differ drastically from those of their crystal counterparts. In many real cases, the materials are only partially disordered as a result of atomic

substitution, elemental non-stoichiometry, fine twinning and small size effects. Depending on the deviations of the real structure from the ideal one, partial disorder can be considered as either weak or strong perturbation. Weak dynamical disorder is always present in any real crystal due to thermal fluctuations.

The disorder in the doped rare earth manganites is expected to vary strongly with doping level and temperature. The dynamical disorder is directly related to such electronic processes as charge hopping and localization in the insulating paramagnetic phase and charge delocalization in the metallic ferromagnetic phase. Therefore, the monitoring of the disorder is of significant interest for understanding the interplay of transport, magnetic and structural properties.

The Raman spectroscopy is an efficient tool for study of structural disorder, including the dynamical one. The first-order Raman phonon spectrum of a nominally perfect crystal consists of series of narrow lines, which correspond to Raman allowed zone-center ( $\Gamma$ -point) phonon modes and obey definite polarization selection rules. The Raman scattering selection rules imposed by the crystal symmetry do not exist in the opposite limit case of amorphous material. The Raman spectrum in this case roughly reflects the one-phonon density-of-states of the crystalline form of the same material. The doped rare earth manganites are an example of partial structural disorder. While the A(La/Ca) and B(Mn) sublattices in a good approximation keep their translational symmetry, the O(oxygen) sublattice is strongly distorted. Compared to the Raman spectra of undistorted material one may expect such implications of partial disorder: (i) broadening of some or all first-order Raman lines; (ii) activation in the Raman spectrum of otherwise forbidden phonon modes; (iii) appearance of additional broad Raman bands of phonon density-of-states origin. It is plausible to assume that the main contribution to

the density-of-states spectral features will come from the most strongly distorted oxygen sublattice.

In the recent years there were numerous reports on the variations of the Raman spectra of  $R_{1-x}^{3+}A_x^{2+}\text{MnO}_3$  ( $R$  = rare earth,  $A$  = Ca, Sr, Ba;  $0 \leq x \leq 1$ ) with  $x$ , and temperature [2, 3, 4, 5, 6, 7, 8]. As a rule, the Raman spectra of doped manganites consist of 2 or 3 broad bands at positions close to those of the strongest Raman lines for the parent orthorhombic  $\text{RMnO}_3$  compounds with  $Pnma$  structure. On the basis of this closeness, the broad bands in the Raman spectra of doped manganites have usually been assigned to the corresponding Raman modes in the  $Pnma$  structure [6]. Alternatively, the broad bands have also been assigned to two-phonon scattering [2] or activation of otherwise forbidden Raman modes.

In this Letter we analyze the Raman spectra of doped manganites in order/disorder terms. On the example of  $\text{La}_{1-x}\text{Ca}_x\text{MnO}_3$  ( $0 \leq x \leq 1$ ) in close comparison with other related materials we argue that the Raman spectra reflect in a unique way the structural disorder induced by the non-coherent Jahn-Teller distortions, as well as its variations with  $x$  and temperature.

The samples and the experimental setups used to obtain the experimental spectra of  $\text{YMnO}_3$  ( $Pnma$ ),  $\text{LaMnO}_3$  ( $Pnma$ ),  $\text{LaMnO}_3$  ( $R\bar{3}c$ ),  $\text{La}_{1-x}\text{Ca}_x\text{MnO}_3$ , and  $\text{CaMnO}_3$  ( $Pnma$ ) are described elsewhere [8, 9, 10, 11, 12]. The calculation of the PDOS and partial PDOS was performed using a shell model of the lattice dynamics developed for  $\text{LaMnO}_3$  [9]. The sampling was carried out over 30000 points in the irreducible wedge of the orthorhombic or rhombohedral Brillouin zone. In the case of the partial PDOS, only modes with predominant oxygen participation were considered.

$\text{LaMnO}_3$  contains only  $\text{Mn}^{3+}$  ions. Below the high-T "orthorhombic-cubic" JT transition ( $T_{JT} \sim 700-750$  K) a cooperative JT distortion of the  $\text{MnO}_6$  octahedra develops due to ordering of  $\text{Mn}^{3+} e_g$  orbitals [15]. The JT distortions are compatible with the orthorhombic ( $Pnma$ ) crystallographic structure and therefore no disorder effects are expected for stoichiometric samples. The Raman spectra of orthorhombic  $\text{LaMnO}_3$  are well known [9]. The most intensive lines at  $612 \text{ cm}^{-1}$  ( $B_{2g}$ ),  $\sim 490 \text{ cm}^{-1}$  ( $A_g$ ), and  $\sim 285 \text{ cm}^{-1}$  ( $A_g$ ) (see Fig.1) correspond to stretching, bending and rotational oxygen vibrations, respectively. These Raman lines are broader than in the isostructural  $\text{YMnO}_3$  and their width and position vary in the spectra reported by different groups [2, 6, 7, 8]. This indicates larger deviation of the real structure of nominally stoichiometric  $\text{LaMnO}_3$  from the ideal  $Pnma$  structure.

As illustrated in Fig.1, the substitution of Ca for La changes drastically the Raman spectra of  $\text{La}_{1-x}\text{Ca}_x\text{MnO}_3$ . For  $x < 0.5$  the spectra in the paramagnetic phase are characterized by two rather broad ( $\sim 100 \text{ cm}^{-1}$ ) high frequency bands centered at  $\sim 500$  and  $\sim 600 \text{ cm}^{-1}$  and a narrower ( $15-20 \text{ cm}^{-1}$ ) low frequency peak. The latter is shifted towards lower wavenumber

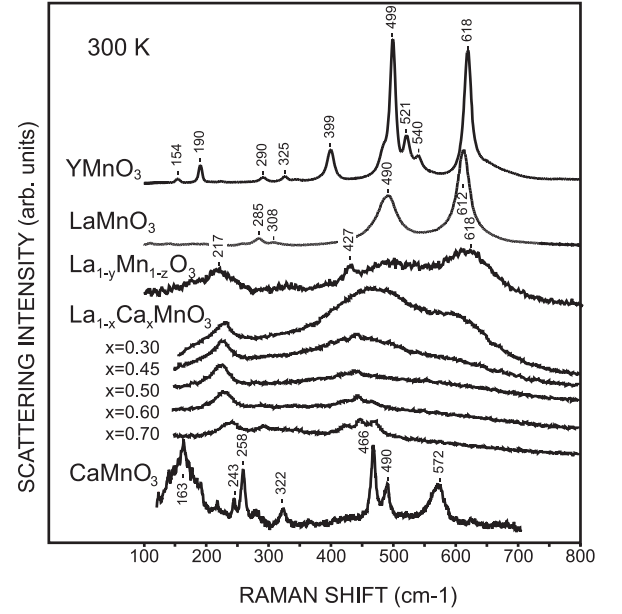


FIG. 1: Comparison of the Raman spectra of  $\text{YMnO}_3$ ,  $\text{LaMnO}_3$ ,  $\text{La}_{1-y}\text{Mn}_{1-x}\text{O}_3$ ,  $\text{La}_{1-x}\text{Ca}_x\text{MnO}_3$  ( $x = 0.3, 0.45, 0.5, 0.6, 0.7$ ) and  $\text{CaMnO}_3$  at room temperature

compared to the corresponding peak of  $\text{LaMnO}_3$  since the frequency of this mode is strongly sensitive to the tilt angle of  $\text{MnO}_6$  octahedra [10]. Remarkably, such lineshape of the Raman spectra is characteristic not only for the  $\text{La}_{1-x}\text{Ca}_x\text{MnO}_3$ , which remain orthorhombic over the whole  $0 \leq x < 0.5$  range. Similar spectra exhibit  $\text{La}_{1-x}\text{Sr}_x\text{MnO}_3$ , which undergo orthorhombic-to-rhombohedral transition at  $x \approx 0.1$ , as well as nominally undoped rhombohedral  $\text{LaMnO}_3$  [10] and cation deficient  $\text{La}_{1-y}\text{Mn}_{1-x}\text{O}_3$  [8]. What these materials have in common is the disorder of oxygen sublattice due to either coexistence of  $\text{Mn}^{3+}$  and  $\text{Mn}^{4+}$  or non-compatibility of Jahn-Teller distortions with the rhombohedral structure. As the transformation of the relatively sharp Raman lines (corresponding to oxygen  $\Gamma$ -point vibrations) to broad bands correlates with occurrence of oxygen disorder, it is reasonable to assign the latter bands to disorder induced scattering. Similar disorder effect occurs in stoichiometric orthorhombic  $\text{LaMnO}_3$  at high temperatures. Indeed, the Raman spectra of  $\text{LaMnO}_3$  at 520 and 720 K [14] are almost identical to these of  $\text{La}_{0.7}\text{Ca}_{0.3}\text{MnO}_3$ .

It is generally accepted that the spectral lineshape of disorder induced Raman scattering qualitatively reflects the phonon density-of-states (PDOS) versus phonon energy distribution for the perfect crystal. Shuker and Gammon [13] have shown that the Raman spectrum  $I(\omega)$  of a disordered material can be approximated by:

$$I(\omega) = \sum_b C_b [n(\omega, T) + 1] \rho_b(\omega) \omega^{-1} \quad (1)$$

where  $\rho_b(\omega)$  is the density of vibrational states in band  $b$  and  $n(\omega, T)$  is the Bose factor. The factors  $C_b$  con-

tain the polarization dependence of scattering and allow different vibrational bands to couple with varying strength to the radiation. If all band couple equally to the incident light  $C_b = C$ , the reduced Raman spectrum  $I'(\omega) = I(\omega)\omega[n(\omega, T) + 1]^{-1} = C\rho(\omega)$  is directly related to the total phonon density-of-states  $\rho(\omega)$

A comparison of the partial (oxygen) PDOS profiles for orthorhombic and rhombohedral  $\text{LaMnO}_3$ , as obtained from lattice dynamical calculations (Fig.2, top panels), with the Raman spectra of  $\text{La}_{0.7}\text{Ca}_{0.3}\text{MnO}_3$  ( $Pnma$ ) and  $\text{LaMnO}_3(R\bar{3}c)$  (Fig.2, bottom panels), assumed to be dominated by disorder scattering features, shows that the experimentally observed bands are much broader than the calculated widths of the phonon branches, involving oxygen motions. The width of the PDOS maxima, however, can be fitted to that of the Raman bands by replacing the PDOS  $\rho(\omega)$  by smeared PDOS

$$\rho_s(\omega) = \int_{-\infty}^{\infty} S(\gamma, \omega - \omega') \rho(\omega') d\omega' \quad (2)$$

and varying the width  $\gamma$  of the smearing function  $S(\gamma, \omega - \omega')$ . The smearing of vibrational frequency is due to finite vibrational time and therefore it is reasonable to use as a smearing function the Lorentzian

$$S(\gamma, \omega - \omega') = \frac{1}{\pi} \frac{\tau}{1 + \tau^2(\omega - \omega')^2} \quad (3)$$

with halfwidth  $\gamma = 1/\tau$ .

The smeared PDOS profiles, shown in Fig.2, correspond to the smeared partial PDOS functions calculated with  $\gamma = 20, 40, 60$  and  $80 \text{ cm}^{-1}$ , respectively. For  $\gamma = 40 \text{ cm}^{-1}$  there is good correspondence between the position and width of the main maxima of PDOS and the experimental Raman spectra. The difference in relative intensities of the maxima of the so calculated PDOS and Raman spectra as well as some shift of the maxima is not unexpected. It reflects the fact that electron-phonon interaction is not the same for the different phonon branches. The parameter  $\tau$  has the clear physical meaning of mean phonon lifetime. It is determined by the scattering rate from (quasi)static lattice distortions ( $1/\tau_d$ ), other phonons ( $1/\tau_{anh}$ ) and the time between two consequent hops ( $\tau_h$ ) as the acts of scattering and atomic rearrangement interrupt the coherency of atomic vibrations. In the case of static or quasistatic disorder  $\tau_d \ll \tau_h$  and  $\tau_d \ll \tau_{anh}$ . The latter relation is justified by the much smaller Raman line widths for ordered orthorhombic  $\text{YMnO}_3$ ,  $\text{LaMnO}_3$ , and  $\text{CaMnO}_3$ . Therefore,

$$\gamma = \frac{1}{\tau} = \frac{1}{\tau_d} + \frac{1}{\tau_{anh}} + \frac{1}{\tau_h} \quad (4)$$

is governed mainly by the lattice distortions.

It is reasonable to expect that the intensity of disorder-induced Raman structures in rare earth manganites will depend on both doping level and temperature. Doping increases the relative volume of distorted areas, thus the

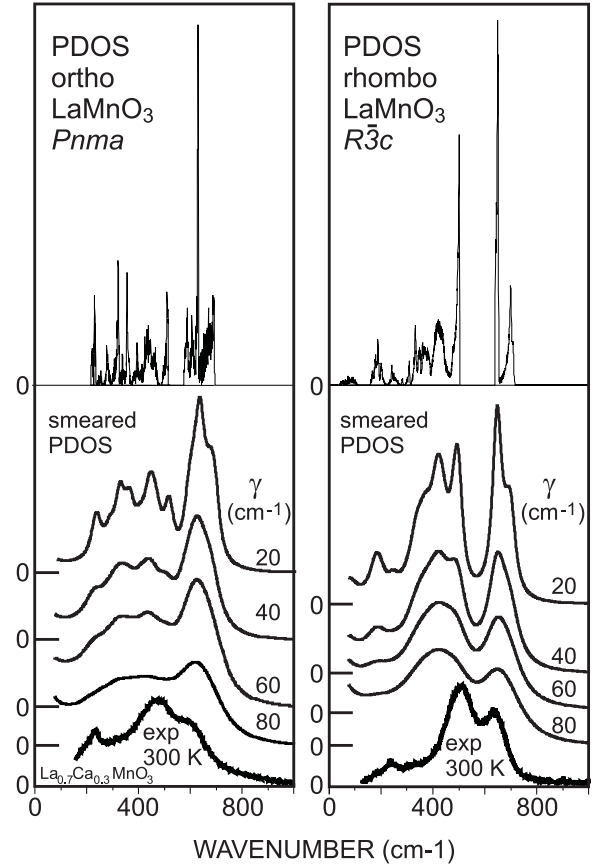


FIG. 2: Comparison of partial PDOS (top panels) and smeared partial PDOS for  $\gamma = 20, 40, 60$ , and  $80 \text{ cm}^{-1}$  (middle panels) of orthorhombic (left) and rhombohedral (right)  $\text{LaMnO}_3$  with experimental Raman spectra of orthorhombic  $\text{La}_{0.7}\text{Ca}_{0.3}\text{MnO}_3$  and rhombohedral  $\text{LaMnO}_3$ .

contributions to the Raman spectra of spectral structures of PDOS origin. For the orthorhombic ( $Pnma$ ) materials the increase with  $x$  of the distorted volume and PDOS bands is accompanied by broadening of the strong lines corresponding to  $\Gamma$ -point Raman modes. The distorted volume reaches its maximum for disordered  $\text{Mn}^{3+}/\text{Mn}^{4+}$  composition with  $\sim 30\%$   $\text{Mn}^{4+}$ . As pointed first by Goodenough [15], this is the disordered composition with the largest number of  $\text{Mn}^{3+}$  ions with one and only one  $\text{Mn}^{4+}$  nearest neighbor. Fig.1 demonstrates that in the insulating phase, the intensity of the density-of-states bands does decrease for  $x > 0.3$ . The decrease in intensity of the disorder-induced bands at higher doping levels and appearance of some sharp Raman features, can also be explained by increasing volume of domains with short-range charge and orbital ordering (COO) [11].

The single act of  $\text{Mn}^{3+} \rightarrow \text{Mn}^{4+}$  hop is much faster than the time of atomic rearrangement caused by the charge transfer. The Jahn-Teller distortion develops (at  $\text{Mn}^{3+}$ ) or disappears (at  $\text{Mn}^{4+}$ ) after some delay time  $\tau_{JT}$ , which can reasonably be approximated by the period of Jahn-Teller-like phonon vibration,  $\approx 10^{-13} - 10^{-14} \text{ sec}$ .

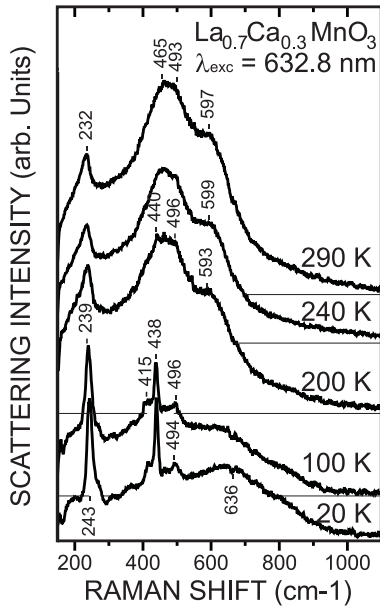


FIG. 3: Variation with temperature of the Raman spectra of  $\text{La}_{0.7}\text{Ca}_{0.3}\text{MnO}_3$  ( $T_c = 200$  K).

Given the mean lifetime  $\tau_h$  of Mn in  $+3$  state between two subsequent  $\text{Mn}^{+3} \rightarrow \text{Mn}^{+4}$  hops remains much larger than  $\tau_{JT}$ , the dynamical Jahn-Teller distortions can be treated as quasistatic with respect to the Raman scattering processes. Therefore, the Jahn-Teller-disorder-induced Raman bands, if observed, will be practically temperature-independent in the whole temperature range, where the relation

$$\tau_{anh} \gg \tau_h \gg \tau_{JT} \approx 10^{-13} - 10^{-14} \text{ sec}, \quad (5)$$

is satisfied and the Jahn-Teller distortions are not coherent. For the doped rare earth manganites this is fulfilled in the paramagnetic and antiferromagnetic insulating phases at doping levels  $x < 0.5$ .

In two limit cases the above relation is no more valid.  $\tau_h$  strongly decreases (i) below the insulator-to-metal transition of CMR materials and (ii) at high temperatures, above the Jahn-Teller transition. As  $\tau_h$  approaches  $\tau_{JT}$  ( $\tau_h > \tau_{JT}$ ), the latter term in Eq.(4) becomes comparable to the former, which results in increase of  $\gamma$ . At  $\tau_h \leq \tau_{JT}$  the Jahn-Teller distortion cannot develop or only partly develops in the time frame of the  $\text{Mn}^{3+}$  state. Physically, this results in strong reduction or disappearance of the Jahn-Teller effect and related non-coherent lattice distortions. This disorder-order transition, concomitant to the paramagnetic-to-ferromagnetic and insulator-metal transitions is reflected in the Raman spectra by disappearance of the broad Jahn-Teller-distortion-induced bands and appearance of much sharper Raman lines, corresponding to the  $\Gamma$ -point Raman phonons of the ordered structure. Fig.3 illustrates such kind of behavior on the example of  $\text{La}_{0.7}\text{Ca}_{0.3}\text{MnO}_3$  ( $T_c = 200$  K). Remnants of the broad Jahn-Teller bands, still observed below  $T_c$  in many occasions, indicate phase separation or inhomogeneous doping. This opens a new way to control the real structure of CMR materials at a microscopic level.

### Acknowledgments

This work is supported in part by the state of Texas through the Texas Center for Superconductivity and Advanced Materials.

- 
- [1] G. Burns and A. M. Glazer, *Space Groups for Solid State Scientists*, Academic Press, New York, 1993.
  - [2] V. B. Podobedov, A. Weber, D. B. Romero, J. P. Rice, and H. D. Drew, *Solid State Comm.* **105**, 589 (1998); *Phys. Rev. B* **58**, 43 (1998).
  - [3] S. Yoon, H. L. Liu, G. Shollerer, S. L. Cooper, P. D. Han, D. A. Payne, S.-W. Cheong, and Z. Fisk, *Phys. Rev. B* **58**, 2795 (1998).
  - [4] E. Granado, N. O. Moreno, A. Garcia, J. A. Sanjurjo, C. Rettori, I. Torriani, S. B. Oseroff, J. J. Neumeier, K. J. McClellan, S.-W. Cheong, and Y. Tokura, *Phys. Rev. B* **58**, 11 435 (1998).
  - [5] M. V. Abrashev, V. G. Ivanov, M. N. Iliev, R. A. Chakalov, R. I. Chakalova, and C. Thomsen, *Phys. Status Solidi B* **215**, 631 (1999).
  - [6] E. Liarokapis, Th. Leventouri, D. Lampakis, D. Palles, J. J. Neumeier, and D. H. Goodwin, *Phys. Rev. B* **60**, 12 758 (1999).
  - [7] P. Björnsson, M. Rübhausen, J. Bäckström, M. Käll, S. Eriksson, J. Eriksen, and L. Börjesson, *Phys. Rev. B* **61**, 1193 (2000).
  - [8] M. N. Iliev, A. P. Litvinchuk, M. V. Abrashev, V. G. Ivanov, H. G. Lee, W. H. McCarroll, M. Greenblatt, R. L. Meng, and C. W. Chu, *Physica C* **341-348**, 2257 (2000).
  - [9] M. N. Iliev, M. V. Abrashev, H. -G. Lee, V. N. Popov, Y. Y. Sun, C. Thomsen, R. L. Meng, and C. W. Chu, *Phys. Rev. B* **57**, 2872 (1998).
  - [10] M. V. Abrashev, A. P. Litvinchuk, M. N. Iliev, R. L. Meng, V. N. Popov, V. G. Ivanov, R. A. Chakalov, and C. Thomsen, *Phys. Rev. B* **59**, 4146 (1999).
  - [11] M. V. Abrashev, J. Bäckström, L. Börjesson, M. Pissas, N. Kolev, and M. N. Iliev, *Phys. Rev. B* **64**, 144429 (2001).
  - [12] M. V. Abrashev, J. Bäckström, L. Börjesson, V. N. Popov, R. A. Chakalov, N. Kolev, R.-L. Meng, and M. N. Iliev, *Phys. Rev. B* **65**, 184301 (2002).
  - [13] R. Shuker and W. W. Gammon, *Phys. Rev. Lett.* **25**, 222 (1970).
  - [14] E. Granado, J. A. Sanjurjo, C. Rettori, J. J. Neumeier, and S. B. Oseroff, *Phys. Rev. B* **62**, 11304 (2000).
  - [15] J. Goodenough, *Phys. Rev.* **100**, 564 (1955).